

Thermal behavior analysis of the solidification of nanoparticle-enhanced phase change material in a latent heat storage system

R. Elbahjaoui*, H. El Qarnia

Cadi Ayyad University, Faculty of Sciences Semlalia, Department of Physics, P.O 2390, Fluid Mechanics and Energetic Laboratory (affiliated to CNRST, URAC 27), Marrakesh, Morocco

*
Email: radouane.elbahjaoui@ced.uca.ac.ma

Abstract

The present work aims to investigate the solidification process of a nanoparticle-enhanced phase change material (NEPCM) filled in a rectangular latent heat storage unit (LHSU). The storage unit consists of several identical slabs filled with n-octadecane as a phase change material (PCM) dispersed with high conductivity nanoparticles (copper). The NEPCM slabs are vertically oriented and separated by rectangular channels in which circulates water as a heat transfer fluid (HTF). A two-dimensional model has been developed and validated by experimental, theoretical and numerical data available in literature. The enthalpy porosity method was adopted for modeling the phase change process. The finite volume approach was used to discretize the resulting equations. The numerical investigations were carried out to investigate the effect of the volumetric fraction of nanoparticles on the heat transfer enhancement during discharging process.

Keywords: *Nanoparticle-enhanced phase change material (NEPCM), nanoparticles, Phase change material (PCM), Latent heat storage unit (LHSU), Solidification.*

1. Introduction

Among of the most preferable techniques for storing solar thermal energy is the latent heat storage (LHS) using phase change materials (PCMs). These materials are able to absorb and release high thermal energy during the melting and solidification processes at a nearly constant temperature. However, the main drawback of the latent heat storage is the low thermal conductivity of PCMs, which leads to the decrease of the heat storage/release rates. To overcome this drawback, several methods have been suggested in the literature including the use of nanoparticle-enhanced phase change materials (NEPCMs), integration of metal matrix in PCMs, use of multiple PCMs and porous matrix.

The melting and solidification processes are encountered in a wide range of applications such as electronic cooling, solar water heating systems and building

envelopes. Therefore, a number of numerical, analytical and experimental studies on latent heat storage units (LHSUs) have been performed over the last 20 years. Charvát et al. [1] numerically and experimentally investigated the thermal performance of a latent heat storage unit composed of 100 aluminum panels filled with paraffin-based PCM and separated by rectangular channels in which circulates air acting as a heat transfer fluid. A 1D simulation model has been developed and validated to numerically investigate the thermal behavior of the storage unit. Bechiri and Mansouri [2] conducted an analytical study on the thermal performance of a LHSU consisting of various flat slabs of PCM charged and discharged by laminar HTF flow circulating between the flat slabs. The results reported that the developed exact solution provides a good estimation of thermal behavior of the storage unit. De Gracia et al. [3] developed a numerical model based the finite volume approach to investigate the thermal performance and behavior of a space cooling system. The studied storage system consists of several PCM panels placed in a ventilated double skin façade. The numerical results show that the ventilated double skin façade with PCM can furnish a net savings of energy exceeding 1.2 MJ. Osterman et al. [4] conducted a numerical and experimental investigations on the thermal performance of a thermal energy storage system used paraffin RT22HC as a phase change material (PCM) to reduce the energy consumption in buildings. The results reveal that the largest savings in winter are in March, while the large amount of accumulated cold in summer is in July. Mosaffa et al. [5] conducted a numerical study to investigate the thermal performance enhancement of a multiple PCM-based free cooling system consisting of several PCM slabs separated by rectangular channels in which circulates air as a HTF. The coefficient of performance (COP) and energy storage effectiveness are defined and used to optimize the free cooling system. Elbahjaoui et al. [6, 7] numerically investigated the effect of the dispersion of high conductive alumina nanoparticles in a base PCM on the thermal performance and flow characteristics of a rectangular LHSU during

melting process. The storage unit consists of a number of vertical and identical slabs filled with nanoparticle-enhanced phase change material (NEPCM) separated by rectangular channels in which circulates water as a HTF. The results reveal that the dispersion of high conductive nanoparticles reduces the PCM melting time.

In the proposed study, the solidification of nanoparticle-enhanced phase change material filled in vertical slabs taking into account the effect of the natural convection is numerically investigated. The solidification process of NEPCM slabs is effected through a cold HTF (water) which circulates in laminar flow between the slabs.

2. Problem Formulation and Numerical Procedure

The LHSU under investigation consists of several rectangular slabs filled with a mixture of Paraffin wax P116 and Al₂O₃ nanoparticles, as shown in Fig. 1a. Water flows in the gap between the slabs and discharges NEPCM. The height and depth of the LHSU are H and e (e = 1m), respectively. The thickness of the NEPCM slabs and water gap are d and w, respectively. The investigation of the whole system can be reduced to the study of a typical and repetitive volume of the unit chosen by symmetry as shown in Fig. 1b.

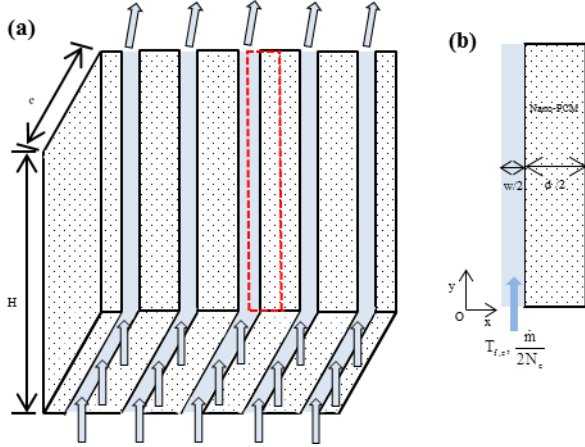


Figure 1: Schematic of the LHSU (a) and computational domain (b).

The transient two-dimensional governing equations can be presented as below [7]:

For NEPCM

$$\frac{\partial U}{\partial X} + \frac{\partial V}{\partial Y} = 0 \quad (1)$$

$$\frac{\partial U}{\partial \tau} + \frac{\partial UU}{\partial X} + \frac{\partial VU}{\partial Y} = -\frac{\partial P}{\partial X} + \frac{\partial}{\partial X} \left(\text{Pr}_m \bar{v}_{nm} \frac{\partial U}{\partial X} \right) + \frac{\partial}{\partial Y} \left(\text{Pr}_m \bar{v}_{nm} \frac{\partial U}{\partial Y} \right) - \bar{C} \frac{(1-f)^3}{(f^3 + b)} U \quad (2)$$

$$\frac{\partial V}{\partial \tau} + \frac{\partial UV}{\partial X} + \frac{\partial VV}{\partial Y} = -\frac{\partial P}{\partial Y} + \frac{\partial}{\partial X} \left(\text{Pr}_m \bar{v}_{nm} \frac{\partial V}{\partial X} \right) + \frac{\partial}{\partial Y} \left(\text{Pr}_m \bar{v}_{nm} \frac{\partial V}{\partial Y} \right) - \bar{C} \frac{(1-f)^3}{(f^3 + b)} V + \text{Ra Pr}_m \bar{\beta}_{nm} \theta_{nm} \quad (3)$$

$$\frac{\partial(\theta_{nm})}{\partial \tau} + \frac{\partial(U\theta_{nm})}{\partial X} + \frac{\partial(V\theta_{nm})}{\partial Y} = \frac{\partial}{\partial X} \left(\bar{\alpha}_{nm} \frac{\partial \theta_{nm}}{\partial X} \right) + \frac{\partial}{\partial Y} \left(\bar{\alpha}_{nm} \frac{\partial \theta_{nm}}{\partial Y} \right) - \frac{1}{\text{Ste}} \frac{\partial f}{\partial \tau} \left(\frac{1-\phi}{1+\phi(\bar{\rho}_n \bar{c}_{p,n} - 1)} \right) \quad (4)$$

For HTF

$$\frac{\partial \theta_f}{\partial \tau} + \frac{\partial(V_f \theta_f)}{\partial Y} = \frac{\partial}{\partial X} \left(\bar{\alpha}_f \frac{\partial \theta_f}{\partial X} \right) + \frac{\partial}{\partial Y} \left(\bar{\alpha}_f \frac{\partial \theta_f}{\partial Y} \right) \quad (5)$$

where f stands for the liquid fraction, ϕ is the volumetric fraction of nanoparticles, U and V are the velocity components, Ste represents the Stefan number, Ra is the Rayleigh number, Pr is the Prandtl number, θ is the dimensionless temperature and $\bar{\alpha}$ represents the dimensionless thermal diffusivity. The subscripts f, m, nm and n stand for HTF, PCM, NEPCM and nanoparticles, respectively.

The initial and boundary conditions of the present LHSU are expressed as follows:

$$\tau = 0: \theta_{nm} = \theta_f = \theta_i, U = V = 0 \quad (6a)$$

$$X = 0: \frac{\partial \theta_f}{\partial X} = 0 \quad (6b)$$

$$X = \frac{\bar{w}}{2}: \bar{k}_f \frac{\partial \theta_f}{\partial X} = \bar{k}_{nm} \frac{\partial \theta_{nm}}{\partial X} \quad (6c)$$

$$Y = 0: \theta_f = -1, \frac{\partial \theta_{nm}}{\partial Y} = 0, U = V = 0 \quad (6d)$$

$$X = \frac{\bar{w}}{2} + \frac{\bar{d}}{2}: \frac{\partial \theta_{nm}}{\partial x} = 0, U = 0, \frac{\partial V}{\partial X} = 0 \quad (6e)$$

$$Y = \bar{H}: \frac{\partial \theta_f}{\partial Y} = \frac{\partial \theta_{nm}}{\partial Y} = 0, U = V = 0 \quad (6f)$$

The governing equations subject to the previous mentioned boundary and initial conditions are discretized using a finite volume approach. The convective terms in governing equations are treated by adopting the power law scheme. The SIMPLE algorithm is used to examine the pressure-velocity coupling in momentum equations. The resulting algebraic equations are solved through the Tri-Diagonal Matrix Algorithm (TDMA).

3. Results and Discussions

The liquid fraction contours and structure of liquid NEPCM flow field at $\tau = 3.24 \times 10^{-2}$, 1.0×10^{-1} , 1.49×10^{-1} and 3.576×10^{-1} are shown in Figs. 2(a)-(d) and 3(a)-(d) for $\phi = 0\%$ and 8% , respectively. As the cold HTF begins to flow between the slabs, a fraction of heat lost by the superheated liquid NEPCM is transmitted by forced convection to HTF and causing, therefore, the start of solidification process. At the early stage ($\tau = 3.24 \times 10^{-2}$), the solid-liquid interface develops close to the heat exchange wall between HTF and NEPCM. Its shape is substantially planar in the down part of the slab and slightly curved in the upper part. In fact, the solidification front moves slowly in the upper part of NEPCM slab. This behavior is due to the natural convection movement which transports the hot liquid

NEPCM to the upper part of the slab. In addition, the effect of natural convection is represented by a single counterclockwise cell formed in the liquid NEPCM zone as shown in Figs. 2(a) and 3(a). As time goes on, the solid fraction increases and the solid-liquid interface moves gradually to the far right side of the NEPCM slab. Simultaneously, the coverage area and the strength of the counterclockwise cell gradually decrease over time. It is interesting to note that the solidification front moves to the far right side faster for the nanoparticles' volumetric fraction $\phi = 8\%$, and the solid fraction augments as the volumetric fraction of nanoparticles increases.

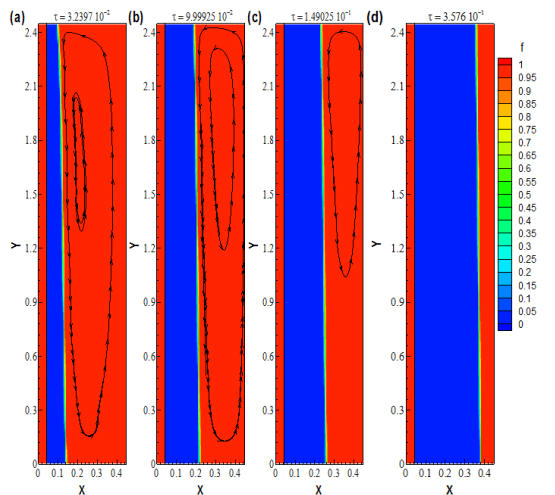


Figure 2: Liquid fraction contours at (a) $\tau = 3.24 \times 10^{-2}$, (b) 1.0×10^{-1} , (c) 1.49×10^{-1} and (d) 3.576×10^{-1} for $\phi = 0\%$

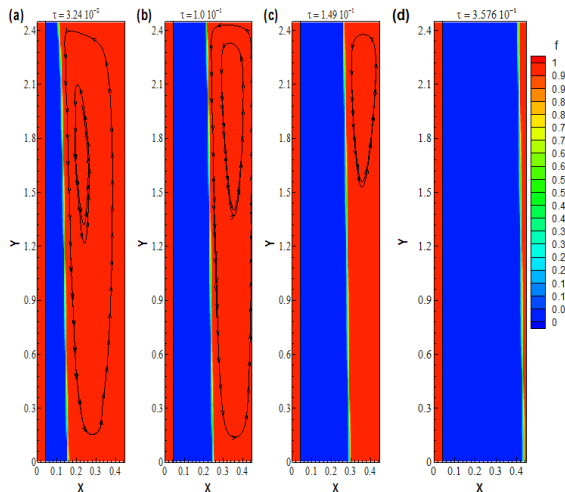


Figure 3: Liquid fraction contours at (a) $\tau = 3.24 \times 10^{-2}$, (b) 1.0×10^{-1} , (c) 1.49×10^{-1} and (d) 3.576×10^{-1} for $\phi = 8\%$

The effect of the volumetric fraction of nanoparticles on the time-wise variation of the liquid fraction is shown in Fig. 4. The liquid fraction decreases over time to reach the zero value when the NEPCM becomes completely solid. During its time evolution, the liquid fraction is lower for high volumetric fraction of nanoparticles due to the enhancement of the thermal conductivity of NEPCM. The solidification time of NEPCM is $\tau = 0.576$, 0.536 and 0.436 for $\phi = 0\%$, 2% and 8% , respectively.

Therefore, it can be revealed that the augmentation of the volumetric fraction of nanoparticles reduces the time required for the complete solidification of NEPCM.

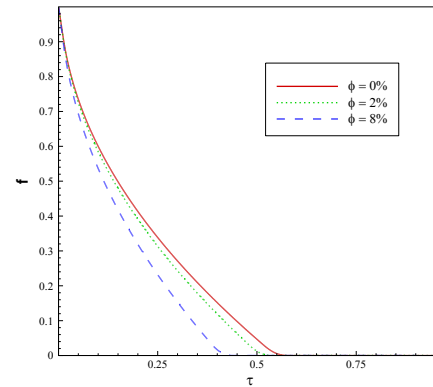


Figure 4: Time-wise variation of the liquid fraction for different nanoparticles' volumetric fractions

4. Conclusion

In the present study, a numerical analysis of the solidification of NEPCM in a rectangular latent heat storage unit heated by a laminar HTF flow is conducted. The numerical calculations were carried out to investigate the effects of the volumetric fraction of nanoparticles (copper) on the thermal performance of the storage unit. The results reveal that the dispersion of nanoparticles enhances the heat transfer rate and therefore reduces the solidification time of NEPCM.

Références

- [1] P. Charvát, L. Klimeš, M. Ostrý, Numerical and experimental investigation of a PCM-based thermal storage unit for solar air systems, *Energy and Buildings*, 68, Part A (2014) 488-497.
- [2] M. Bechiri, K. Mansouri, Exact solution of thermal energy storage system using PCM flat slabs configuration, *Energy Conversion and Management*, 76 (2013) 588-598.
- [3] A. De Gracia, L. Navarro, A. Castell, L.F. Cabeza, Energy performance of a ventilated double skin facade with PCM under different climates, *Energy and Buildings*, 91 (2015) 37-42.
- [4] E. Osterman, V. Butala, U. Stritih, PCM thermal storage system for 'free' heating and cooling of buildings, *Energy and Buildings*, 106 (2015) 125-133.
- [5] A.H. Mosaffa, C.A. Infante Ferreira, F. Talati, M.A. Rosen, Thermal performance of a multiple PCM thermal storage unit for free cooling, *Energy Conversion and Management*, 67 (2013) 1-7.
- [6] R. Elbahjaoui, H.E. Qarnia, M.E. Ganaoui, Melting of nanoparticle-enhanced phase change material inside an enclosure heated by laminar heat transfer fluid flow, *Eur. Phys. J. Appl. Phys.*, 74 (2016) 24616.
- [7] R. Elbahjaoui, H. El Qarnia, Transient behavior analysis of the melting of nanoparticle-enhanced phase change material inside a rectangular latent heat storage unit, *Applied Thermal Engineering*, 112 (2017) 720-738.